PHYSICAL REVIEW E VOLUME 61, NUMBER 1 JANUARY 2000

Density correlations in lattice gases in contact with a confining wall

J. Reinhard, W. Dieterich, and P. Maass
Fakultät für Physik, Universität Konstanz, D-78457 Konstanz, Germany

H. L. Frisch
Department of Chemistry, University of Albany, State University of New York, Albany, New York 12222

(Received 17 August 1999)

A discrete version of classical density functional theory applicable to lattice gases or Ising spin systems is proposed, which accounts for the requirement of particle-hole symmetry in the presence of pairwise forces. Results of our theory for density profiles and two-particle correlation functions in two-dimensional strip geometries compare favorably with Monte Carlo simulations. Some problems with standard ''weighted-density'' approximation schemes, when applied to lattice gases, are pointed out.

PACS number(s): 61.20.−p, 05.50.+q, 68.35.−p

I. INTRODUCTION

In recent years, density functional theory (DFT) has been developed sufficiently far to become a quantitative, microscopic method in studies of the equilibrium properties of nonuniform fluids [1,2]. In numerous applications the DFT has proved not only to account for the gas-liquid and the freezing transition in the bulk of three-dimensional (3D) fluids [3–9], but also for various phenomena at surfaces and in systems with restricted geometries. Examples are surface enrichment in mixtures [10], wetting phenomena [11], and phase transitions in fluids confined between hard walls [12] and in narrow pores [13] as well as two-dimensional melting [14]. The DFT thus appears to constitute a quite general tool in the investigation of small confined systems, which is a problem of growing interest in view of the potential technological importance of artificial nano-sized structures.

Most of the underlying models are naturally formulated in continuous space. There are, however, important physical situations, e.g., metallic alloys or submonolayer adsorbate systems, suggesting a coarse-grained description in terms of discrete molecular configurations. This poses the problem of formulating a discrete analog of density functional theory, based on a lattice gas Hamiltonian of the form

$$\mathcal{H}=\frac{1}{2}\sum_{ij} V_{ij}n_i n_j+\sum_i (\epsilon_i-\mu)n_i, \tag{1}$$

where the occupation numbers for lattice sites i are denoted by n_i. In a ''fermionic'' lattice gas, which we consider here, a site is either vacant ($n_i=0$) or singly occupied ($n_i=1$), so that $n_i^2=n_i$. In Eq. (1), V_{ij} are the two-particle interaction parameters, ϵ_i the site energies due to an external potential, and μ is the chemical potential. As shown previously, all formal steps in DFT for continuous fluids are readily adapted to the discrete case described by Eq. (1) [15]. The central feature of the lattice version of DFT is a variational principle based on the grand free energy

$$\Omega_\epsilon[\mathbf{p}]=\sum_i (\epsilon_i-\mu)p_i+F[\mathbf{p}] \tag{2}$$

as a functional of the average occupation numbers $\mathbf{p}=\{p_i\}$; $p_i=\langle n_i\rangle$. The free-energy functional $F[\mathbf{p}]$, which is independent of ϵ_i, can be decomposed into an ''ideal'' part which describes a noninteracting lattice gas,

$$F_{id}[\mathbf{p}]=k_BT\sum_i [p_i\ln p_i+(1-p_i)\ln(1-p_i)], \tag{3}$$

and an excess part $F_{exc}[\mathbf{p}]$ due to interactions. For a given temperature T, chemical potential μ, and external potential ϵ_i, the equilibrium occupation is obtained by minimizing $\Omega_\epsilon[\mathbf{p}]$, the minimum value representing the thermodynamical grand free energy. The condition $\partial\Omega_\epsilon/\partial p_i=0$ immediately yields an expression of the type of a Fermi-Dirac distribution,

$$p_i=(1+\exp\{\beta(\epsilon_i-\mu)-c_i^{(1)}[\mathbf{p}]\})^{-1}, \tag{4}$$

with the ''correlation potential''

$$-k_BTc_i^{(1)}[\mathbf{p}]=\partial F_{exc}/\partial p_i. \tag{5}$$

In order to proceed, one needs an approximation for $c_i^{(1)}[\mathbf{p}]$ or $F_{exc}[\mathbf{p}]$. The simplest approximation, analogous to the freezing theory of Ramakrishnan and Yussuoff [16], consists of an expansion of $F_{exc}[\mathbf{p}]$ up to terms of second order in the deviations $p_i-\overline{p}$ from some uniform reference density $\overline{p}$,

$$F_{exc}[\mathbf{p}]\simeq-\frac{k_BT}{2}\sum_{ij} c_{ij}(\overline{p})(p_i-\overline{p})(p_j-\overline{p}). \tag{6}$$

Here $c_{ij}(p)$ denotes the Ornstein-Zernike direct correlation function, assumed to be known. It is related to the pair correlation function

$$H_{ij}(p)=\langle n_i n_j\rangle-p^2 \tag{7}$$

by the Ornstein-Zernike (OZ) relation, which in our discrete theory can be written in the form

$$H_{ij}(p)=p(1-p)\left[\delta_{ij}+\sum_k c_{ik}(p)H_{kj}(p)\right]. \tag{8}$$

©2000 The American Physical Society

Within the above scheme, ordering transitions in lattice gases can be treated in analogy to the freezing transition in conventional DFT for continuous fluids [15]. In addition, the discrete DFT has successfully been applied to interfacial properties in lattice gases, including the thermodynamics of stepped surfaces and surface roughening [17]. More recently it has been shown to account also for surface segregation effects in fcc alloys [18]. However, all practical calculations performed so far made use of the approximation (6), which is clearly insufficient for a treatment of some important circumstances. For example, it fails to account for any realistic bulk phase diagram in the presence of competing interactions and, generally, for surface phase diagrams including wetting phenomena [19]. Dealing with these problems requires terms higher than second order in F_{exc}. Truncated higher-order expansions of F_{exc} in powers of the density inhomogeneities, however, may lead to intricate problems of convergence [20]. In continuum theories, various forms of the ''weighted-density approximation'' (WDA) [1], which formally involve powers in the density inhomogeneities to infinite order, have been developed in treatments of the freezing transition [3–9], interfacial properties and wetting phenomena [21,22], capillary condensation [13], particle density profiles of hard spheres at hard walls [23,24], triplet direct correlations in homogeneous fluids [24,25], and pair correlations of hard spheres near planar walls [26] and in slit geometries [27].

By immediately applying standard WDA schemes (which involve only one weight function) to the lattice gas, however, one is faced with the problem of incorporating particle-hole symmetry. This symmetry is an inherent property of the Hamiltonian (1) based on pairwise interactions. While this problem is discussed in some detail in the Appendix, we pursue a different line in the main part of this paper. We propose and analyze a simple form for the free-energy functional which preserves particle-hole symmetry and simultaneously constitutes an important conceptual and practical improvement over the ''linear DFT'' scheme contained in Eq. (6).

Our paper is organized as follows. In Sec. II we introduce our basic approximation, whose structure is closely related to the work by Götzelmann *et al.* [26], and which we call ''semilinear DFT.'' In Sec. III we apply it to a two-dimensional lattice gas with attractive nearest-neighbor interactions in a strip geometry, where the confining walls exert a potential ϵ_W to their adjacent (outermost) layer. As usual, we need the direct correlation function for uniform states as our basic input. This quantity is obtained from the Ornstein-Zernike equation in connection with the Kramers-Wannier approximation, which allows us to compare the semilinear DFT with Monte Carlo simulations in a quantitative manner. Besides the calculation of density profiles, our main concern is two-point correlation functions, describing density correlations which are parallel and perpendicular to the confining walls. Generally, these correlation functions directly enter the cross section in surface scattering experiments [28]. A detailed Monte Carlo study of density patterns and two-point density correlations of Ising systems in strip and film geometries has been published before by Binder *et al.* [10], whereas correlations of inhomogeneous hard-core systems have been treated by Robledo [29] for the discrete case and Götzelmann *et al.* [26] for continuous fluids. Section IV summarizes our results.

II. SEMILINEAR DFT

Let us first of all assess the behavior of the excess free-energy functional $F_{exc}[\mathbf{p}]$ with respect to the exchange of particles and holes (vacancies). Clearly, the expression

$$\sum_{ij} V_{ij} n_i n_j - V_0 \sum_i n_i \tag{9}$$

with $V_0 = \Sigma_j V_{ij}$ is invariant if we replace n_i with $1-n_i$ on every site i. Since the form of the functional $F_{exc}[\mathbf{p}]$ is determined only by the pair interactions but is independent of the single-particle terms in Eq. (1), it follows that the functional

$$F_{exc}^{(S)}[\mathbf{p}] = F_{exc}[\mathbf{p}] - \frac{1}{2} V_0 \sum_i p_i , \tag{10}$$

which is F_{exc} minus the average of the second term in Eq. (9), does not change with respect to the replacement $p_i \rightarrow 1 - p_i$. Note that $F_{exc}^{(S)}[\mathbf{p}]$ is zero for both a completely empty and a completely filled lattice. Correspondingly, if $f_{exc}(p)$ denotes the excess free energy per site in a homogeneous phase with average density *p*, the function

$$f_{exc}^{(S)}(p) = f_{exc}(p) - \frac{1}{2} V_0 p \tag{11}$$

obeys the symmetry relation

$$f_{exc}^{(S)}(p) = f_{exc}^{(S)}(1-p). \tag{12}$$

Before we introduce our basic approximation to $F_{exc}[\mathbf{p}]$, consider the representation

$$-\beta f_{exc}(p) = \int_0^p dp' \int_0^{p'} dp'' \tilde{c}_0(p'') \tag{13}$$

of $f_{exc}(p)$ in terms of the zero wave-vector component $\tilde{c}_0(p) = \Sigma_j c_{ij}(p)$ of the direct correlation function. Together with the symmetry relation (12) and

$$c_{ij}(p) = c_{ij}(1-p), \tag{14}$$

Eq. (13) yields a condition for $\tilde{c}_0(p)$ worth noting. Since $f_{exc}^{(S)}(0) = f_{exc}^{(S)}(1) = 0$, we have $f_{exc}(1) = V_0/2$ which can be combined with Eq. (13) and Eq. (14) to give

$$\int_0^1 dp\, \tilde{c}_0(p) = -\beta V_0 . \tag{15}$$

This sum rule for $\tilde{c}_0(p)$ provides a test for any approximate calculation of $c_{ij}(p)$ in a lattice gas.

Under the assumption that Eq. (15) is satisfied, we now construct an approximate free-energy functional consistent with the symmetry of Eq. (10) under the exchange $p_i \leftrightarrow 1 - p_i$. Writing $F_{exc}^{(S)}[\mathbf{p}] = \Sigma_i f_i^{(S)}$, we require the excess free energy $f_i^{(S)}$ related to site *i* to consist of a local term determined by the exact free energy per site of a uniform state [Eq. (13)], and additive contributions from neighboring sites j, which are *linear* in the occupation differences $p_j - p_i$. Hence,

$$F_{exc}^{(S)}[\mathbf{p}] = \sum_i \left[f_{exc}^{(S)}(p_i) - \frac{k_B T}{2} \sum_{j \neq i} \alpha_{ij}(p_j - p_i) \right]. \tag{16}$$

The p_i-dependent coefficients α_{ij} are determined by requiring that

$$\left(\frac{\partial^2(-\beta F_{exc}^{(S)})}{\partial p_i \partial p_j} \right)_p = c_{ij}(p) \tag{17}$$

hold for uniform states with (arbitrary) constant density p. This gives

$$\alpha_{ij} = \int_{1/2}^{p_i} dp' c_{ij}(p').$$

The advantage of the expression (16) over the ‘‘linear’’ DFT, Eq. (6), is that it involves the correct free energy of uniform states but no particular reference state. The form of Eq. (16) is analogous to that derived in previous work by Götzelmann *et al.* on continuous hard core systems [26]. Their ‘‘linear-weighted density functional theory’’ is based on an expression of the same type as Eq. (16), where the densities p_i and p_j are replaced by weighted densities.

III. MODEL CALCULATIONS IN TWO DIMENSIONS

We now apply the above scheme to particles with nearest-neighbor attraction $V < 0$ on a two-dimensional square lattice. In order to obtain the input quantities $c_{ij}(p)$ for that model, some further approximation is required. We shall use the Kramers-Wannier cluster approximation, in which the elementary squares of the square lattice are used as the basic clusters. This method is known to give a fair representation of the phase diagram of the nearest-neighbor Ising model, and its accuracy is regarded as sufficient for the present purpose [30]. Specifically, it yields a critical temperature given by $k_B T_c^{\mathrm{KW}}/|V| \simeq 0.606$ while the exact critical temperature satisfies $k_B T_c/|V| \simeq 0.567$. From the Kramers-Wannier approximation we obtain the excess free energy $f_{exc}(p)$, which in connection with Eq. (11) satisfies the symmetry condition (12). In addition, by appropriate summations over cluster variables we also obtain the pair-correlation functions $H_{ij}(p)$ for nearest and next-nearest neighbors, denoted by $H_1(p)$ and $H_2(p)$, respectively.

In order to determine the nth-neighbor direct correlation function, denoted by $c_n(p)$, we take advantage of the fact that, generally, $c_{ij}(p)$ becomes very small at distances beyond the interaction range (see, however, Ref. [31]). Hence we take $c_n(p) = 0$ for $n \geqslant 2$ and are left with two unknowns, $c_1(p)$ and $c_0(p) \equiv c_{ii}(p)$. These are determined most easily by using the compressibility sum rule

$$\tilde{c}_0(p) \simeq c_0(p) + 4c_1(p) = -\beta \frac{d^2}{dp^2} f_{exc}(p) \tag{18}$$

and the OZ equation (8) for $i = j$:

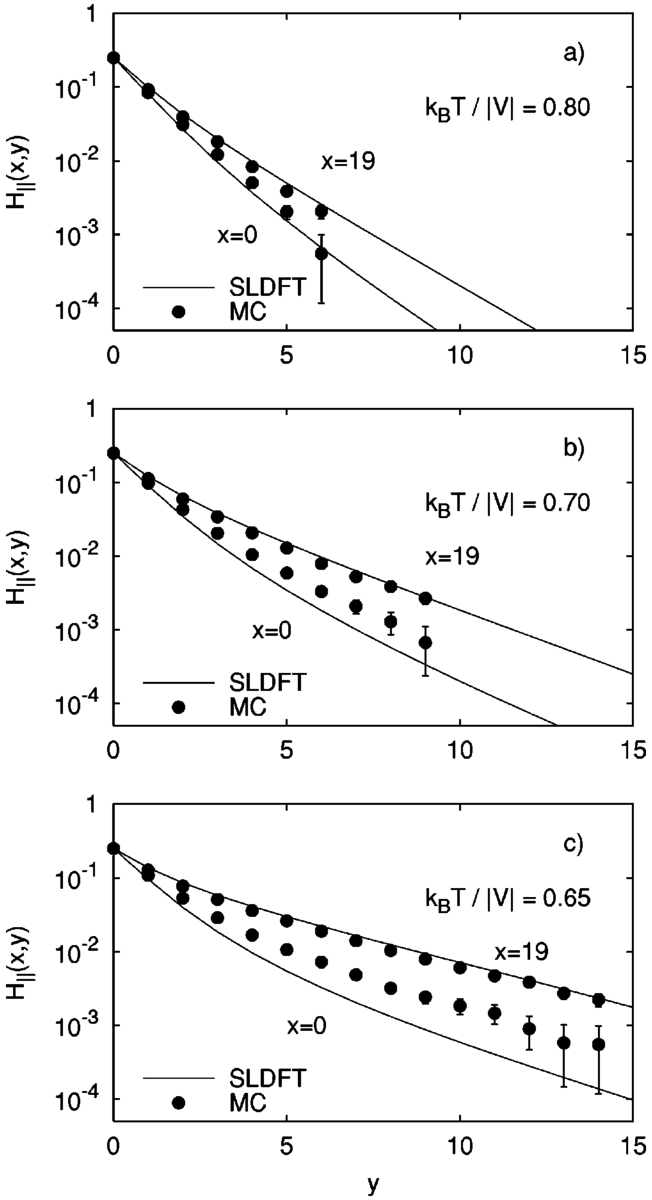

FIG. 1. Lateral pair correlation function $H_{\|}(x,y)$ in a strip of width $L = 40$ versus lateral coordinate y in the first row $(x = 0)$ and far from the wall $(x = 19)$ resulting from Monte Carlo simulations and the semilinear DFT. Energetically neutral walls $(\epsilon_W = 0)$ were assumed, with constant (x-independent) density $p_x = 0.5$.

$$p(1-p)c_0(p) + 4c_1(p)H_1(p) = 0. \tag{19}$$

Here we have used $H_{ii}(p) = p(1-p)$, so that $\Sigma_k c_{ik} H_{ki} = 0$.

The remaining equations (8) $(i \neq j)$ can be used as a consistency check of this procedure. For example, one can calculate $H_2(p)$ in terms of $c_n(p)$ from Eq. (8) by taking Fourier transforms and then compare the result with H_2 obtained directly from the Kramers-Wannier approximation. Calculations show that as long as $k_B T/|V| \gtrsim 0.7$ the difference between both methods amounts to less than 5% for all p, but differences increase at lower temperatures.

Knowing $f_{exc}(p)$ and $c_n(p)$, the excess free-energy functional, Eq. (16), is completely specified and we can now calculate density profiles p_i and pair-correlation functions $\langle n_i n_j \rangle$ for inhomogeneous systems by using Eqs. (4) and (5).

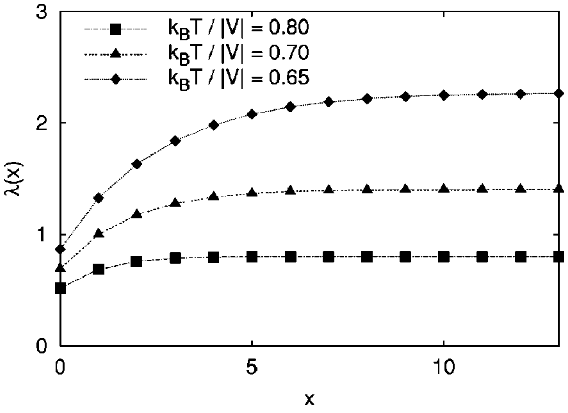

FIG. 2. Decay length $\lambda(x)$, see Eq. (22), of lateral correlations for neutral walls ($p_x=0.5$) and three different temperatures, following from the SLDFT (cf. also Fig. 1).

According to Percus' test-particle method [32], $\langle n_i n_j\rangle/p_j$ with $i\neq j$ is regarded as the density at site i, obtained from Eq. (4), under the condition that a particle is fixed at site j, which means that in solving Eq. (4) for p_i we set $p_j=1$.

In applying this formalism, our primary goal is to investigate wall-induced correlations in confined systems. As an example, we study in the following a strip geometry, where the lattice consists of points $i=(x,y)$ with perpendicular (dimensionless) coordinate $x(0\leqslant x\leqslant L)$ and lateral (dimensionless) coordinate $y(-\infty<y<+\infty)$. Translational invariance is assumed in the direction parallel to the strip. Lateral and perpendicular correlations are characterized by

$$H_{\parallel}(x,y)=\langle n_{x0}n_{xy}\rangle-p_x^2 \tag{20}$$

and

$$H_{\perp}(x)=\langle n_{00}n_{x0}\rangle-p_0p_x, \tag{21}$$

where in the latter case one point is fixed at the surface. For the density profile perpendicular to the walls we have used the notation $p_x=\langle n_{x,y}\rangle$ which in the strip geometry considered is independent of y. Boundary conditions with respect to the x direction are such that occupations outside the strip are purely random with $p_i=0.5$ (which corresponds to zero magnetization in the equivalent Ising model).

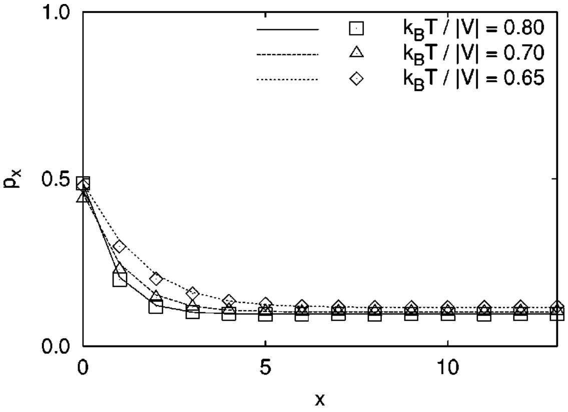

FIG. 3. Density profiles p_x according to the SLDFT (lines) in comparison with MC data (open symbols) for three different cases satisfying $p_0\simeq 0.5$ and $p_x\simeq 0.1$ in the bulk. See Table I for values of ϵ_W and μ.

TABLE I. Parameters used to calculate the density profiles in Fig. 3 and lateral correlations in Fig. 4.

$k_BT/\|V\|$	$\epsilon_W/\|V\|$	$\mu/\|V\|$
0.80	−0.7	−0.4
0.70	−0.4	−0.2
0.65	−0.3	−0.1

To start our discussion, consider a half-filled lattice with constant (zero) site energies. Then for the boundary conditions chosen we simply obtain a constant density $p_x=0.5$ (''neutral'' walls). However, because of the missing neighbors (in the language of Ising spins) at surface sites, correlations among near-surface sites become weaker than in the bulk. This is demonstrated in Fig. 1, which shows the lateral decay of the function $H_{\parallel}(x,y)$ at the surface $(x=0)$ and in the middle $(x=19)$ of a strip of width $L=40$ for several temperatures above the critical temperature T_c. Data points obtained from Monte Carlo simulation are shown for comparison. For temperatures $k_BT/|V|\gtrsim 0.75$ [Fig. 1(a)] good agreement with the semilinear DFT (SLDFT) (solid lines) is found over the main decay of the functions $H_{\parallel}(x,y)$. As expected, at $x=0$ the decay is considerably faster than at $x=19$, where the curves reflect bulk behavior. For lower temperatures [Figs. 1(b) and 1(c)] we still find agreement with Monte Carlo data inside the bulk. However, the DFT underestimates the range of lateral correlations at the surface $x=0$. The reason may be seen in the fact that the influence of the occupational environment on the behavior of the two-particle correlation function is basically a multi- (larger-than-two) particle correlation effect, whose strength is underestimated by the DFT when we approach the critical temperature.

In Fig. 2 we plotted the characteristic length

$$\lambda(x)=\frac{\sum\limits_{y\geqslant 0} yH_{\parallel}(x,y)}{\sum\limits_{y\geqslant 0} H_{\parallel}(x,y)} \tag{22}$$

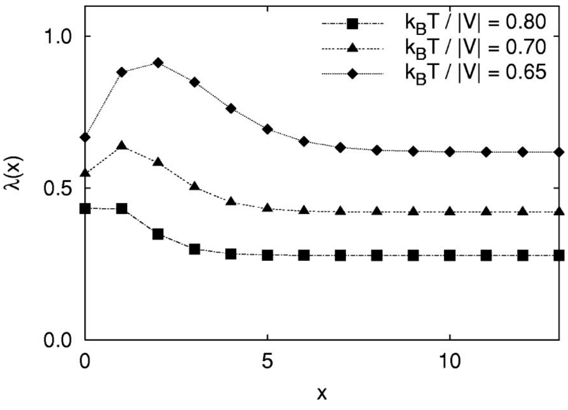

FIG. 4. Decay length $\lambda(x)$ of lateral correlations for the same set of parameters as in Fig. 3 (from SLDFT).

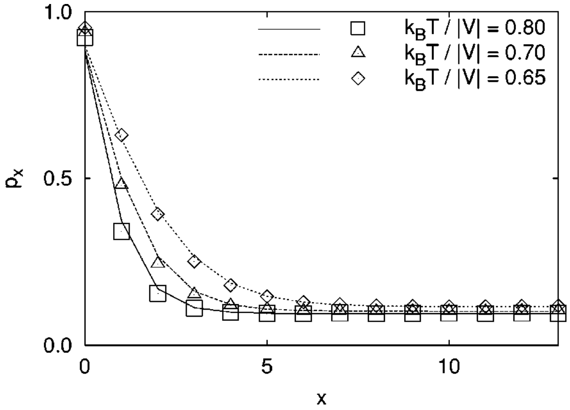

FIG. 5. Same as Fig. 3, but with stronger attraction to the walls, such that $p_0 \simeq 0.9$ (cf. Table II).

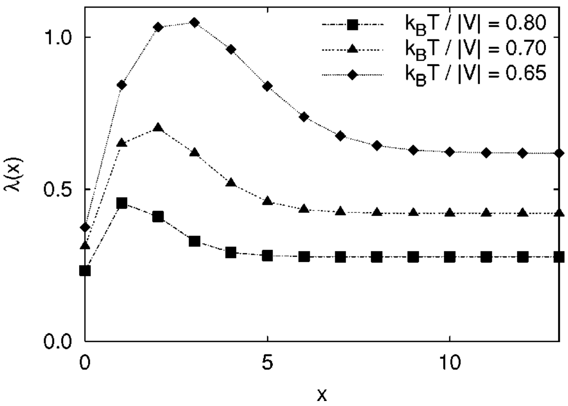

FIG. 6. Decay length $\lambda(x)$ of lateral correlations for the same set of parameters as in Fig. 5 (from SLDFT).

for the lateral decay of the correlation function $H_{\|}(x,y)$, derived from the semilinear DFT for the same set of parameters as in Fig. 1. Inside the bulk, $\lambda(x)$ can be identified with the bulk correlation length ξ, but when moving in the outward direction it substantially decreases in a range $x \lesssim \xi$ near the surface, reflecting weaker correlations. This trend is clearly enhanced as the temperature gets lower.

A quite different situation arises in systems with small bulk occupation, but an attractive interaction with the confining wall. Let us represent this particle-wall interaction by a potential $\epsilon_W < 0$ associated with sites in the outermost rows $x=0$ and $x=L$. For example, choosing the chemical potential μ such that $p_x \simeq 0.1$ in the bulk, a wall energy $\epsilon_W/|V| = -1.2$, and $k_BT/|V| = 0.8$, we obtain an enrichment profile with a density $p_0 \simeq 0.5$ for the outermost row. Profiles calculated from the SLDFT quantitatively agree with corresponding Monte Carlo (MC) data; see Fig. 3. This figure includes two further cases with lower temperatures where in each case μ and ϵ_W are chosen such that $p_0 \simeq 0.5$ and $p_x \simeq 0.1$ in the bulk (see Table I). To discuss correlations, let us note that near the surface the system locally is closer to critical conditions than in the bulk and hence we expect $\lambda(x)$ to increase when approaching the surface. This is confirmed in Fig. 4 again for several temperatures. However, the above-mentioned effect of missing neighbors outside the wall is also visible: at the two lower temperatures the length $\lambda(x)$, after passing through a maximum, becomes smaller when approaching $x=0$.

It is instructive to study cases with an even stronger attraction to the wall, where the density profile p_x passes the value 0.5 already at some distance x_0 from the wall. Situations with $p_x = 0.1$ in the bulk and $p_0 = 0.9$ are presented in Fig. 5 for the same temperatures as in Fig. 3 (for the corresponding values of ϵ_W and μ, see Table II). Again we observe excellent agreement between calculated density profiles and MC data. Clearly, particle-hole symmetry (see Sec. II) is a necessary requirement for any theory capable of describing density profiles of this type. The range of lateral correlations $\lambda(x)$ now is expected to vary with x in a nonmonotonic fashion and to display a maximum near x_0, which is confirmed in Fig. 6 by our calculations based on the SLDFT.

TABLE II. Parameters used to calculate the density profiles in Fig. 5 and lateral correlations in Fig. 6.

$k_BT/\|V\|$	$\epsilon_W/\|V\|$	$\mu/\|V\|$
0.80	-1.9	-0.4
0.70	-1.5	-0.2
0.65	-1.3	-0.1

IV. SUMMARY

A density functional theory for discrete lattice gases with two-particle interactions has been formulated that respects particle-hole symmetry. The theory is based on an approximate free energy per site which contains the local free energy of a homogeneous system and additive terms linear in the occupation of neighboring sites. Within this ''semilinear DFT'' we calculated density profiles and two-point correlation functions for particles subjected to a nearest-neighbor attraction on a two-dimensional square lattice confined between two parallel walls. The required input quantity, the Ornstein-Zernike direct correlation function of the two-dimensional homogeneous lattice gas, was calculated by combining the Kramers-Wannier approximation with the OZ equation. (This procedure may be termed ''Kramers-Wannier closure'' for the OZ equation.)

Good quantitative agreement between calculated density profiles and Monte Carlo simulations has been achieved. In particular we discussed the range of lateral correlations in the presence of different forms of the enrichment profile induced by the walls. For temperatures sufficiently above T_c the lateral correlation functions show satisfactory agreement with simulation data. Our study suggests that the proposed method may serve as a useful tool in studies of real physical systems, e.g., of two-dimensional confined adsorbate systems or of three–dimensional thin films of metallic alloys.

ACKNOWLEDGMENTS

We are grateful for stimulating discussions with P. Nielaba and Y. Rosenfeld. This work was supported in part by the Deutsche Forschungsgemeinschaft, SFB 513. H.L.F. was supported by the NSF Grant No. DMR 962 8224 and the J.S. Guggenheim Foundation. P.M. thanks the Deutsche Forschungsgemeinschaft for financial support.

APPENDIX: WEIGHTED-DENSITY APPROXIMATION SCHEMES FOR LATTICE GASES

WDA methods have become a standard tool in the equilibrium theory of continuous fluids. Numerous applications to the structure of geometrically confined fluids, interfacial properties, and also the freezing transition have successfully been worked out. Yet we would like to point out that one must be careful when adapting this concept to discrete lattice gas models incorporating the site exclusion principle. Consider a lattice gas with two-particle interactions, leaving thermodynamical properties invariant under the exchange of particles and holes. In the spirit of the Curtin-Ashcroft version of the WDA [4], we may choose the following ansatz for the symmetrized functional (10), written in terms of Ising spin variables $s_i = p_i - 1/2$:

$$F_{exc}^{(\mathrm{S})}[\mathbf{s}] - F_{exc}^{(\mathrm{S})}[\mathbf{0}] = \sum_i s_i \Psi(\overline{s_i}), \tag{A1}$$

with $F_{exc}^{(\mathrm{S})}[\mathbf{s}] = F_{exc}^{(\mathrm{S})}[-\mathbf{s}]$ and $F_{exc}^{(\mathrm{S})}[\mathbf{0}]$ being determined by the condition $F_{exc}^{(\mathrm{S})} = 0$ for an empty or a completely filled lattice. The quantity $\Psi(s)$ is defined such that $f_{exc}^{(\mathrm{S})}(0) + s\Psi(s)$ is equal to the symmetrized excess free energy per site of a uniform system with average spin s. Furthermore, $\overline{s_i}$ is a weighted spin,

$$\overline{s_i} = \sum_j w_{ij}(\overline{s_i}) s_i ,$$

with w_{ij} a (translationally invariant) normalized weight function: $\Sigma_j w_{ij} = 1$. Following the standard procedure [4], the condition (17) leads to a first-order differential equation for the Fourier components $\tilde{w}_q(s)$ of the weight function, which is formally equivalent to the Curtin-Ashcroft WDA equation:

$$-k_B T \tilde{c}_q(s) = 2\Psi'(s)\tilde{w}_q(s) + s\frac{d}{ds}\{\Psi'(s)[\tilde{w}_q(s)]^2\}. \tag{A2}$$

Here $\tilde{c}_q(s)$ is the qth Fourier component of the OZ direct correlation function. Since $\tilde{c}_q(s) = \tilde{c}_q(-s)$ and $\Psi(s) = -\Psi(-s)$, Eq. (A2) allows symmetrical solutions $\tilde{w}_q(s) = \tilde{w}_q(-s)$. Note that the physical solution of Eq. (A2) must satisfy $\tilde{w}_{q=0}(s) = 1$, which is the normalization condition. In the case of a half-filled lattice, $s = 0$, we have for the symmetrical solution (assuming differentiability of $[\Psi'\tilde{w}^2]$ at $s = 0$)

$$\tilde{w}_q(0) = -\frac{k_B T \tilde{c}_q(0)}{2\Psi'(0)}, \tag{A3}$$

which can be used as initial condition in the integration of Eq. (A2).

A simplified version of this type of theory is the ‘‘hybrid weighted-density functional approach’’ (HWDA) [23], which in our case yields

$$-k_B T \tilde{c}_q(s) = 2\Psi'(s)\tilde{w}_q(s) + s\Psi''(s)[\tilde{w}_q(s)]^2 \tag{A4}$$

instead of Eq. (A2). Numerical studies reveal that for attractive interaction, $V < 0$, this equation generally does not permit real solutions for all temperatures and densities. Let us illustrate this by considering the dilute limit $s = \pm\frac{1}{2}$ at low temperatures. Using the compressibility sum rule (18), we rewrite Eq. (A4) as

$$-k_B T \tilde{c}_q = 2\Psi'[\tilde{w}_q - \tilde{w}_q^2] - k_B T \tilde{c}_{q=0}\tilde{w}_q^2 . \tag{A5}$$

In the dilute limit the coefficients c_0 and c_1 in Eq. (18) are given by $c_0(\pm\frac{1}{2}) = 0$ and $c_1(\pm\frac{1}{2}) = \exp(-\beta V) - 1$, hence for low temperatures (large β) we have the estimate

$$\left|\tilde{c}_q\left(\pm\frac{1}{2}\right)\right| \propto \exp(-\beta V) - 1 \simeq \exp(\beta|V|), \tag{A6}$$

which will become large for low temperatures. To estimate $\Psi'(\pm\frac{1}{2})$ in Eq. (A5) we observe that Eq. (A1) demands $\Psi(s) = s^{-1}[f_{exc}^{(\mathrm{S})}(s) - f_{exc}^{(\mathrm{S})}(s=0)]$. Using Eqs. (11) and (13), we obtain

$$\Psi'(s = \pm\tfrac{1}{2}) = 4 f_{exc}^{(\mathrm{S})}(s=0) + V_0 = 4 f_{exc}(p = \tfrac{1}{2}).$$

Since for attractive interaction $f''_{exc} = -\beta^{-1}\tilde{c}_0 < 0$, we deduce from Eq. (13) and the fact that $f_{exc}(1) = \frac{1}{2}V_0 < 0$ the inequalities $\frac{1}{2}V_0 p \leqslant f_{exc}(p) \leqslant 0$. Now we have an upper bound for the magnitude of $\Psi'(\pm\frac{1}{2})$ which is independent of temperature:

$$|\Psi'(\pm\tfrac{1}{2})| \leqslant |V_0|.$$

Therefore, in view of Eq. (A6), $|\Psi'(\pm\frac{1}{2})| \ll |\tilde{c}_q(\pm\frac{1}{2})|$ for low temperatures and Eq. (A5) yields

$$[\tilde{w}_q(\pm\tfrac{1}{2})]^2 \simeq \frac{\tilde{c}_q(\pm\frac{1}{2})}{\tilde{c}_{q=0}(\pm\frac{1}{2})}, \tag{A7}$$

which is negative if we choose q near the boundary of the first Brillouin zone of our lattice. A related problem also exists for the differential equation (A2).

This problem does not exist for repulsive interactions, favoring ordered states of the lattice gas. The possibility to investigate ordering transitions in lattice gases by this method still needs to be explored. Note also that Eqs. (A2) and (A4) as used in the WDA and HWDA for continuous fluids reduce to Eq. (A3) in the dilute limit, *not* to Eq. (A7). This is due to the fact that for continuous fluids, the spin density s must be replaced by the particle density p in Eqs. (A2) and (A4).

An alternative expression for $F_{exc}^{(\mathrm{S})}[\mathbf{p}]$ might be

$$F_{exc}^{(\mathrm{S})}[\mathbf{p}] = \sum_i p_i(1-p_i)\Phi(\overline{p_i}), \tag{A8}$$

which in the case of a dilute (or nearly filled) lattice gas should yield properties similar to the continuum theory for a system of particles (or holes). Here $\overline{p_i}$ again is a weighted density, and $\Phi(p) = \Phi(1-p)$. Instead of Eqs. (A2) and (A4) we now obtain

$$\begin{aligned}-k_BT\tilde{c}_q(p)={}&-2\Phi(p)+2(1-2p)\Phi'(p)\tilde{w}_q(p)\\&+p(1-p)\frac{d}{dp}\{\Phi'(p)[\tilde{w}_q(p)]^2\}\end{aligned}\tag{A9}$$

for the WDA and

$$\begin{aligned}-k_BT\tilde{c}_q(p)={}&-2\Phi(p)+2(1-2p)\Phi'(p)\tilde{w}_q(p)\\&+p(1-p)\Phi''(p)[\tilde{w}_q(p)]^2\end{aligned}\tag{A10}$$

for the HWDA. In Eq. (A9), the coefficient of $\tilde{w}_q'$ vanishes for $p=0$ (and $p=1$) as well as for $p=\frac{1}{2}$ (due to the symmetry of Φ). Thus, we have

$$\tilde{w}_q(0)=\frac{2\Phi(0)-k_BT\tilde{c}_q(0)}{2\Phi'(0)}.$$

On the other hand, $\tilde{w}_q(\frac{1}{2})$ is obtained from a quadratic equation as that solution which on continuation to $q=0$ satisfies the normalization condition $\tilde{w}_{q=0}(p)\equiv 1$. Choosing this solution as initial condition to integrate Eq. (A9), the resulting $\tilde{w}_q(p)$ does not converge to $\tilde{w}_q(0)$ on approaching $p=0$ and $p=1$, but diverges. A related problem of the HWDA equation (A10) is that correctly normalized solutions $\tilde{w}_q(p)$ become discontinuous at some density p_*, for any $q\neq 0$. Hence, Eq. (A8) can be used, if at all, only in cases where the densities p_i show little spatial variation and do not come close to p_*.

Basically, the difficulties with the above WDA schemes, Eqs. (A1) and (A8), arise from the fact that by solving the associated first-order differential equation for the weight function, the correct low-density limit and the symmetry condition generally cannot be satisfied simultaneously. However, these shortcomings may not arise in more general WDA methods involving more than one weight function [9,24–26]. Note also that an exact density functional exists for hard rods in one dimension, which involves two different weight functions [33–35].

[1] R. Evans, in *Fundamentals of Inhomogeneous Fluids*, edited by D. Henderson (Dekker, New York, 1992), p. 85.
[2] H. Löwen, Phys. Rep. **237**, 251 (1994).
[3] P. Tarazona, Phys. Rev. A **31**, 2672 (1985).
[4] W.A. Curtin and N.W. Ashcroft, Phys. Rev. A **32**, 2909 (1985); Phys. Rev. Lett. **56**, 2775 (1986).
[5] A.R. Denton and N.W. Ashcroft, Phys. Rev. A **39**, 4701 (1989).
[6] J.F. Lutsko and M. Baus, Phys. Rev. Lett. **64**, 761 (1990).
[7] X.C. Zeng and D.W. Oxtoby, Phys. Rev. A **41**, 7094 (1990).
[8] D.W. Oxtoby, Nature (London) **347**, 725 (1990).
[9] Y. Rosenfeld, M. Schmidt, H. Löwen, and P. Tarazona, J. Phys.: Condens. Matter **8**, L577 (1996).
[10] K. Binder, P. Nielaba, and V. Pereyra, Z. Phys. B: Condens. Matter **104**, 81 (1997).
[11] S. Dietrich, in *Phase Transitions and Critical Phenomena*, edited by C. Domb and J. L. Lebowitz (Academic Press, London, 1987), Vol. 12, pp. 1–218.
[12] M. Schmidt and H. Löwen, Phys. Rev. E **55**, 7228 (1997).
[13] R. Evans, J. Phys.: Condens. Matter **2**, 8989 (1990).
[14] V.N. Ryzhov and E.E. Tareyeva, Phys. Rev. B **51**, 8789 (1995).
[15] M. Nieswand, W. Dieterich, and A. Majhofer, Phys. Rev. E **47**, 718 (1993); **48**, 2521 (1993).
[16] T.V. Ramakrishnan and M. Yussouff, Phys. Rev. B **19**, 2775 (1979).
[17] D. Reinel, W. Dieterich, and A. Majhofer, Phys. Rev. E **50**, 4744 (1994).
[18] C. Seok and D.W. Oxtoby, J. Phys.: Condens. Matter **9**, 87 (1997).
[19] R. Evans, P. Tarazona, and U. Marini Bettolo Marconi, Mol. Phys. **50**, 993 (1983); R. Evans and U. Marini Bettolo Marconi, Phys. Rev. A **34**, 3504 (1986).
[20] W.A. Curtin, J. Chem. Phys. **88**, 7050 (1988).
[21] W.A. Curtin, Phys. Rev. Lett. **59**, 1228 (1987); Phys. Rev. B **39**, 6775 (1989).
[22] R. Ohnesorge, H. Löwen, and H. Wagner, Phys. Rev. E **50**, 4801 (1994).
[23] R. Leidl and H. Wagner, J. Chem. Phys. **98**, 4142 (1993).
[24] E. Kierlik and M.L. Rosinberg, Phys. Rev. A **42**, 3382 (1990).
[25] Y. Rosenfeld, Phys. Rev. Lett. **63**, 980 (1989); J. Chem. Phys. **92**, 6818 (1990).
[26] B. Götzelmann, M. A. Haase, and S. Dietrich, Phys. Rev. E **53**, 3456 (1996).
[27] B. Götzelmann and S. Dietrich, Phys. Rev. E **55**, 2993 (1997).
[28] S. Dietrich and A. Haase, Phys. Rep. **260**, 1 (1995).
[29] A. Robledo, Mol. Phys. **39**, 193 (1980).
[30] Note that conventionally the Ornstein-Zernike relation is solved in connection with some approximate ''closure relation'' between H_{ij} and c_{ij}. One can show, for example, that the Percus-Yevick closure on a lattice, if symmetrized appropriately, yields results similar to the Bethe approximation.
[31] C. Borzi, G. Ord, and J.K. Percus, J. Stat. Phys. **46**, 51 (1987).
[32] J.K. Percus, Phys. Rev. Lett. **8**, 462 (1962).
[33] A. Robledo and C. Varea, J. Stat. Phys. **26**, 513 (1981).
[34] J.K. Percus, J. Chem. Phys. **75**, 1316 (1981); J. Stat. Phys. **28**, 67 (1982).
[35] J. Buschle, P. Maass, and W. Dieterich (unpublished).